AGU PUBLICATIONS

[Earth Surface]

Supporting Information for

[The Fate of Sediment After a Large Earthquake]

[Oliver Francis[1,2,*], Xuanmei Fan[3], Tristram Hales[1,2], Daniel Hobley[2], Qiang Xu[3], Runqiu Huang[3]]

[[1]Sustainable Places Research Institute, Cardiff University, Cardiff, United Kingdom

[2]School of Earth and Environmental Sciences, Cardiff University, Cardiff, United Kingdom

[3]State Key Laboratory for Geohazard Prevention and Geoenvironment Protection, Chengdu University of Technology, Chengdu, China

Corresponding author: Oliver Francis (Oliver.Francis@gfz-potsdam.de)

*Now at Section 4.7: Earth Surface Process Modelling, German Research Centre for Geosciences (GFZ), Potsdam, Germany]

Contents of this file

Introduction

This file including the supporting information for The Fate of Sediment After a Large Earthquake. These support and provide further details of the methods and results described within the main text of the manuscript.

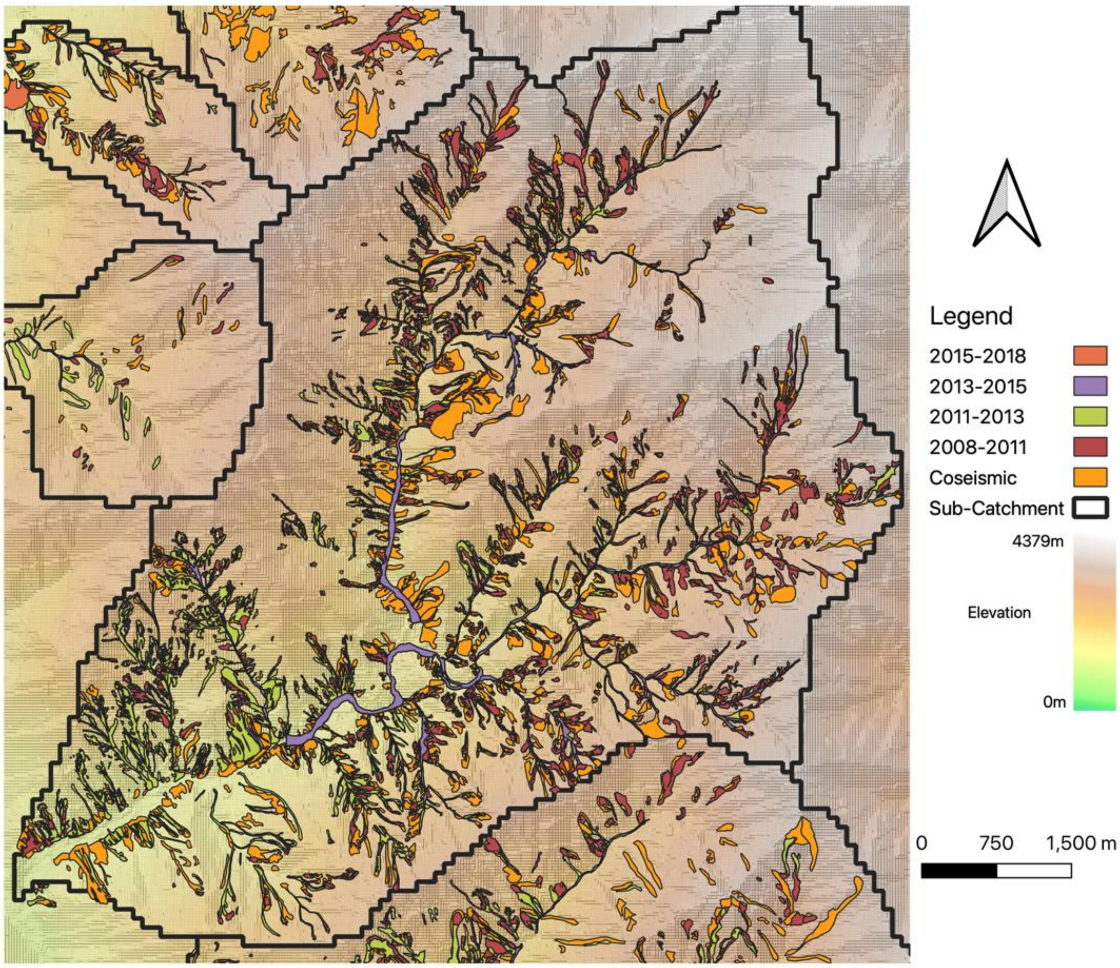

Figure S1: An example of a mapped catchment. Each mass movement is mapped as a polygon which is investigated for each epoch. The mass movement polygons are coloured based upon the epoch they were mapped in. Any mass movement which intersects with a mass movement from a previous epoch is defined as a remobilisation, if it does not intersect any previous mass movements it is defined as new.

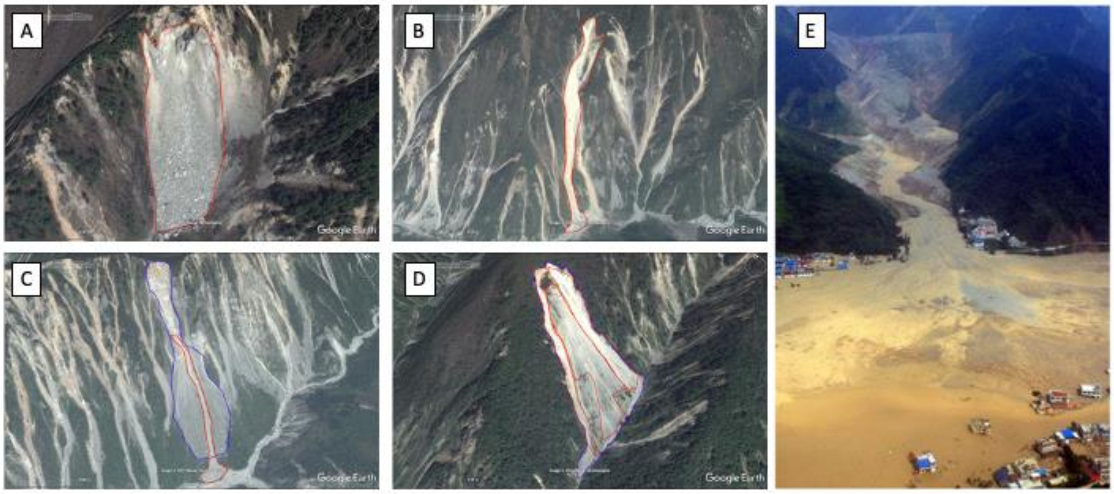

Figure S2: Examples of the main mass movement processes mapped within the mass movement inventory and an example of a catchment clearing debris flow. A) a mapped landslide, B) A mapped debris flow, C) a coseismic landslide which is then remobilised by a channelised remobilisation which deposits sediment into the tributary channels D) a coseismic landslide which is actively being remobilised but there no clear channelisation within the remobilisation. E) is a debris flow that occurred in 2010 which was triggered within coseismic landslide deposits in the Wenjia torrent and deposited over 1,000,000 m^3 of sediment directly into the Min Jiang. A,B,C,D are produced from Google Earth imagery while E is an aerial photo taken from (Tang et al., 2012).

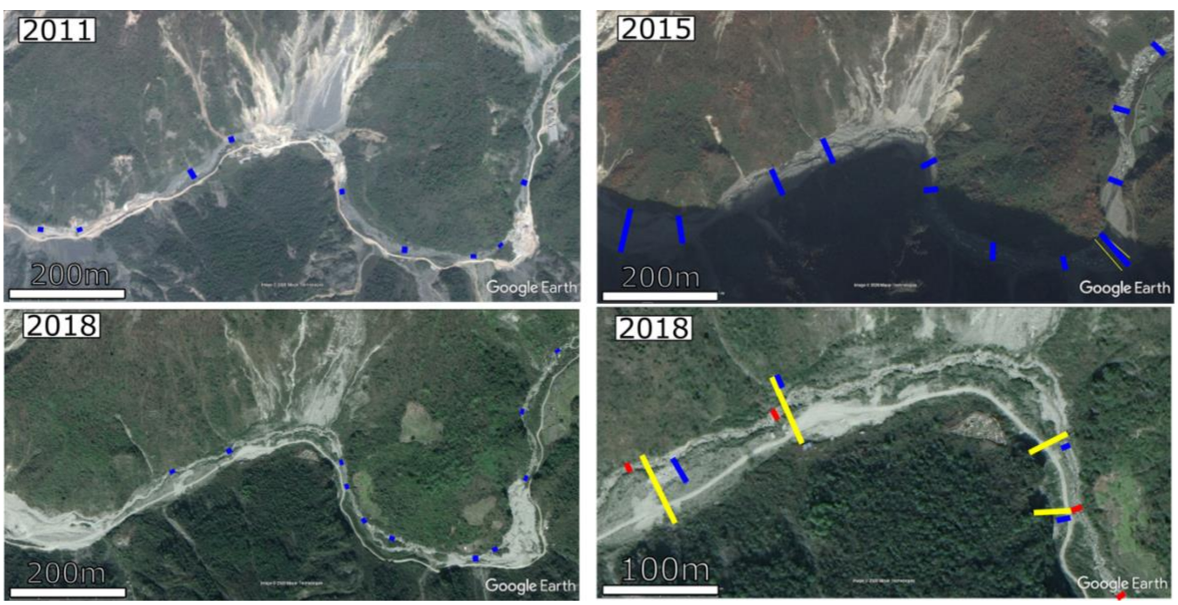

Figure S3: Examples of the mapping of tributary channel deposit cross sections. The first 3 images are of the same area through time. For each image the channel deposit is mapped to the edge of the visible sediment at regular intervals, shown in blue. The final image shows a subsection of a catchment with the mapped cross sections in different colours. The cross section from 2011 is mapped in blue, 2011 in yellow and 2018 in red. Due to rectification errors within Google Earth the cross sections are not in the exact same position, however care was taken to ensure repeat surveys were taken as close as possible.

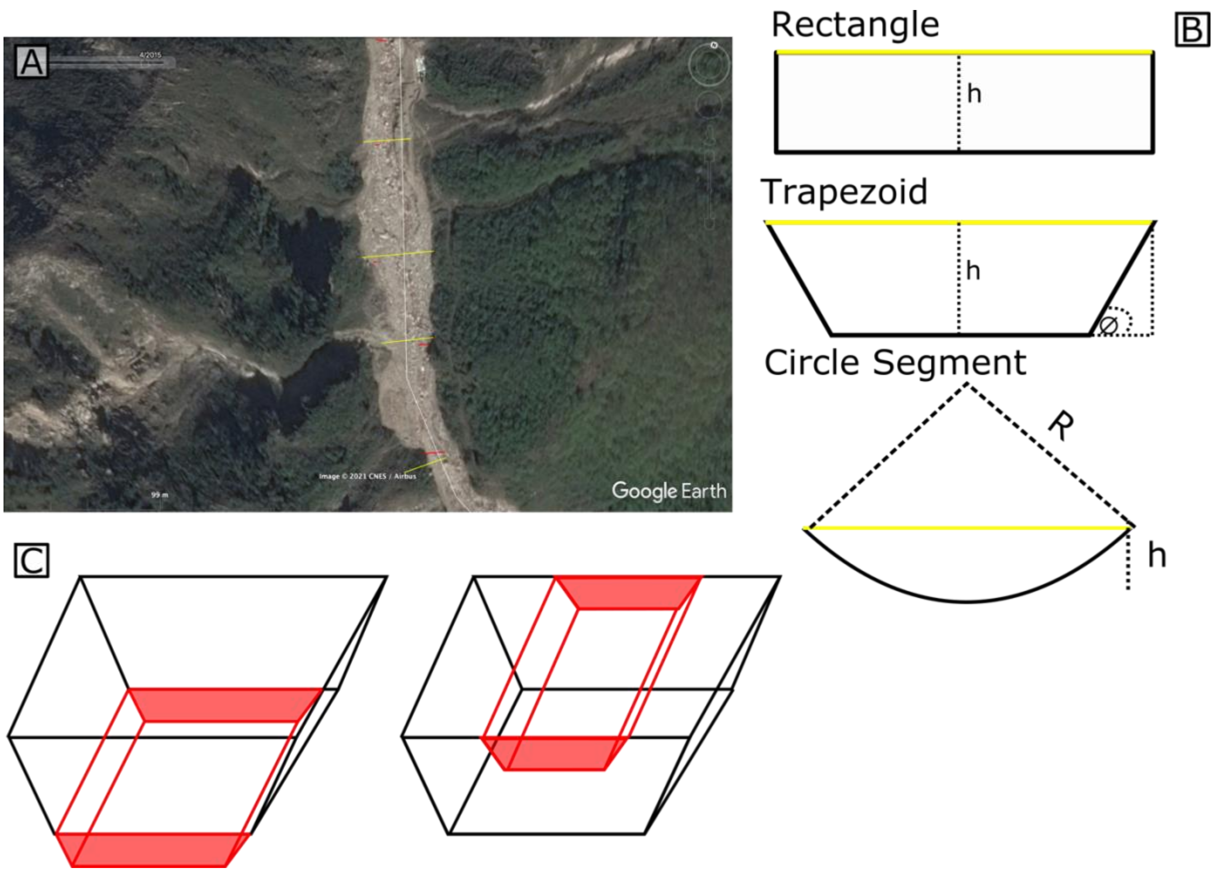

Figure S4: A demonstration of how the volumes of the channel deposits were estimated. A) a section of a surveyed tributary channel, the yellow lines indicate the width of the channel deposit in the year 2015 while red was mapped in 2011. Here each channel width has increased in size. The white line is used to estimate the distance between each channel width. B) The different shapes used for the cross-sectional area. The height of the rectangle and trapezoid was estimated by the width scaling ratio of (Moody & Troutman, 2002) $h=0.27(w^2/7.2^2)^{0.39}$. Simple trigonometry and angle relationships were used to determine the lengths of unknown sections. C) An example of how volume changes were estimated, if the width increases we estimate the volume deposited on top of the previous width (red), if the width remains the same we estimate the volume of sediment removed by the incision of the active channel which is reworking the sediment (shaded red). The volume is calculated by multiplying the added or removed cross sectional area by the distance between the measured widths.

Date of image	Source of Image	Resolution	Coverage
May – July 2008	Aerial photography	1 – 2.5m	97%

April 2011	Aerial photography and Worldview satellite	0.5 – 1m	99%
April 2013	Aerial photography and Pleiades satellite	0.5 - 2m	95%
April 2015	Spot 6 satellite	1.5m	99%
April 2017	Spot 6 satellite	3m	93%
April 2018	Spot 6 satellite	3m	93%

Table S1. The date, source and resolution of the images used in the development of the inventory. Coverage describes the percentage of the study area covered by the imagery at each time step.

Change in tributary channel deposits = New debris flows + Channelised remobilistation + Unchannelised remobilisation + Overland flow erosion – Incision – Suspended sediment – (0.5×Catchment clearing debris flows)	Equation 1
Debris flows (Channelised remobilisation + New debris flows) = Change in tributary channel deposits + Suspended sediment + Incision + (0.5×Catchment clearing debris flows) - Overland flow erosion – Unchannelised remobilisation	Equation 2

Table S2. The sediment budget of the tributary channel deposits and the equation used for determining the volume of the sediment mobilised by debris flows.

Frequency per year	2008	2011	2013	2015	2018
New hillslope deposits (debris flows)	462	24	20	4.5	0
New hillslope deposits (landslides)	8225	142	83.5	6.5	2.3
New tributary channel deposits	108	2.7	5	1	0
New Min Jiang deposits	35	0	0	0	0
Channelised remobilisation into the tributary channel deposits	0	112.3	67	16.5	1.6
Unchannelised remobilisation into the tributary channel deposits	0	200.7	92	10.5	3.6
Remobilised into the Min Jiang	0	4.3	4.5	0	0
Catchment clearing debris flows	23	37.3	5.5	0	0

Table S3. The average frequency of mapped mass movements for each mapped epoch. The number of catchment clearing debris flows is derived from (Fan et al., 2019)

References:

Fan, X., Scaringi, G., Domènech, G., Yang, F., Guo, X., Dai, L., He, C., Xu, Q., & Huang, R. (2019). Two multi-temporal datasets that track the enhanced landsliding after the 2008 Wenchuan earthquake. *Earth System Science Data*, *11*(1), 35–55. https://doi.org/10.5194/essd-11-35-2019

Moody, J. A., & Troutman, B. M. (2002). Characterization of the spatial variability of channel morphology. *Earth Surface Processes and Landforms*, *27*(12), 1251–1266. https://doi.org/10.1002/esp.403

Tang, C., Van Asch, T. W. J., Chang, M., Chen, G. Q., Zhao, X. H., & Huang, X. C. (2012). Catastrophic debris flows on 13 August 2010 in the Qingping area, southwestern China: The combined effects of a strong earthquake and subsequent rainstorms. *Geomorphology*, *139–140*(August 2010), 559–576. https://doi.org/10.1016/j.geomorph.2011.12.021